

# CONTROLLING THE SPIN POLARIZATION OF THE ELECTRON CURRENT IN A SEMIMAGNETIC RESONANT-TUNNELING DIODE

N.N. Beletskii<sup>1,2</sup>, G.P. Berman<sup>2</sup>, and S.A. Borysenko<sup>1</sup>

<sup>1</sup>*Usikov Institute of Radiophysics and Electronics of the National Academy of Sciences of Ukraine,  
12, Acad. Proskura Str., 61085 Kharkov, Ukraine and*

<sup>2</sup>*Theoretical Division, MS B213, Los Alamos National Laboratory, Los Alamos, New Mexico 87545*

The spin filtering effect of the electron current in a double-barrier resonant-tunneling diode (RTD) consisting of  $\text{Zn}_{1-x}\text{Mn}_x\text{Se}$  semimagnetic layers has been studied theoretically. The influence of the distribution of the magnesium ions on the coefficient of the spin polarization of the electron current has been investigated. The dependence of the spin filtering degree of the electron current on the external magnetic field and the bias voltage has been obtained. The effect of the total spin polarization of the electron current has been predicted. This effect is characterized by total suppression of the spin-up component of electron current, that takes place when the Fermi level coincides with the lowest Landau level for spin-up electrons in the RTD semimagnetic emitter.

PACS numbers: 75.50.Pp, 72.25.Dc, 72.25.Hg, 72.10.-d

## Introduction

Spin-polarized ballistic electron transport in resonant-tunneling semimagnetic semiconductor nanostructures attracts considerable attention of the researchers developing the fundamentals of spintronics [1, 2, 3, 4, 5, 6, 7, 8]. This transport is also associated with the search for effective sources of the spin-polarized current which can be controlled using a constant magnetic field  $\mathbf{B}$  as well as by means of a bias voltage  $V_a$ . Resonant-tunneling semimagnetic nanostructures are characterized by the high degree of the current spin polarization due to the  $sp-d$  exchange interaction between the conduction electrons and localized electrons of the magnetic ions belonging to the semimagnetic semiconductors [9, 10, 11]. In

a magnetic field  $\mathbf{B}$ , this interaction gives rise to the giant Zeeman splitting of the electron energy levels. As a result, the electrons with spins oriented along  $\mathbf{B}$  (spin-up electrons) and against  $\mathbf{B}$  (spin-down electrons) move in different potential fields and have different transmission coefficients through the resonant-tunneling semimagnetic semiconductor nanostructures. Therefore, spin filtering of the electron current occurs even in moderate magnetic fields, and the electrons with a certain spin direction dominate in the current. The presence of the spin filtering of the electron current can be detected by its injection into a light-emitting diode and by the measurement of the electromagnetic radiation of the circular polarization [12, 13].

The idea of using semimagnetic semiconductors for spin filtering of the electron current has been proposed in [4]. It was shown that the electron current flowing through a semimagnetic semiconductor layer in a constant magnetic field of 2-4 T displays a high degree of spin polarization. In [5], the dependences of the coefficient of current spin polarization on the thickness of the semimagnetic layer and the bias voltage have been investigated. In [6, 7], the results of papers [4, 5] have been summarized for the case of a nanostructure consisting of two semimagnetic semiconductor layers separated by a non-magnetic layer. In these papers along with the study of voltage-current characteristics of the nanostructure, the influence of the thicknesses of semimagnetic layers [6] and operating temperatures [7] on the value of the coefficient of the current spin polarization has been investigated.

Later, it was shown that the degree of the current spin polarization can be enhanced if the resonant-tunneling nanostructure has semimagnetic contacts [8]. This is related to the fact that the conduction band edge of a semimagnetic emitter in the magnetic field  $\mathbf{B}$  is spin-dependent. In this case, the number of spin-down electrons in the emitter exceeds the number of spin-up electrons. As a result, spin-down electrons play the determining role in the current flowing through the resonant-tunneling nanostructure with semimagnetic contacts. Thus, the spin-dependent shift of the conduction band edge of the semimagnetic emitter and the spin-dependent electron transmission through semimagnetic layers lead to a significant increase in the coefficient of current spin polarization in fully semimagnetic resonant-tunneling nanostructures.

In this paper new results are presented on the theory of the effect of the electron current spin filtering in a double-barrier resonant-tunneling diode (RTD) based on a  $\text{Zn}_{1-x}\text{Mn}_x\text{Se}$  semimagnetic semiconductor. The choice of this semimagnetic semiconductor is related to

the presence of an RTD in which the emitter, collector, and quantum well consist of this semiconductor material [3]. In contrast to the paper [8], we assume that all RTD layers are semimagnetic. Moreover, in our paper the value of the electron current density and the coefficient of current spin polarization are determined taking into account the influence of the bias voltage  $V_a$  on the coefficient of the electron transmission through the RTD.

The dependencies of the electron current density and the coefficient of the current spin polarization on the constant magnetic field  $\mathbf{B}$  as well as on a bias voltage  $V_a$  are studied for different spatial distributions of magnetic ions in the RTD and for different values of the Fermi level in the RTD emitter. The occurrence of the total polarization of the electron current has been predicted. Total polarization takes place when the Fermi level coincides with the lowest Landau level for spin-up electrons in the RTD semimagnetic emitter.

### Theoretical model

We assume that the RTD (including its emitter and collector) consists of  $\text{Zn}_{1-x_j}\text{Mn}_{x_j}\text{Se}$  layers with different Mn concentrations  $x_j = \{x_1, x_2, x_3, x_4, x_5\}$  (Fig.1a). The region  $z < z_1$  is an RTD emitter and the region  $z > z_4$  is a RTD collector. We assume that the emitter and collector are  $n$ -doped. The external magnetic field  $\mathbf{B}$  is directed along the  $z$  axis. The bottoms of the conduction bands for the spin-down and spin-up electrons are shown by the solid and dashed lines correspondingly in Fig.1b. The values of  $L_i = z_{i+1} - z_i$  ( $i = 1, 2, 3$ ) are the thicknesses of two potential barriers ( $L_1$  and  $L_3$ ) and potential well ( $L_2$ ) of the RTD. The value  $E_F$  is the Fermi level in the emitter and collector.

As is well known, the band gap of semimagnetic semiconductors depends on the Mn concentration [9, 14, 15, 16]. Therefore at the boundary between two semimagnetic semiconductors with different Mn concentrations, an offset of the band gap takes place. In this case, one part of this offset falls at the conduction band offset and the other one falls at the valence band offset [14]. At low temperatures the band gap  $E_{gj}$  of the semimagnetic semiconductors depends slightly on  $x_j$  in the range  $x_3 < 0.065$  [9, 14, 15, 16]. Therefore, to obtain the dependence of the conduction band edge  $E_{cj}(x_j)$  of the semimagnetic semiconductor, we use the following empirical formula which describes the experimental dependencies in [14]:

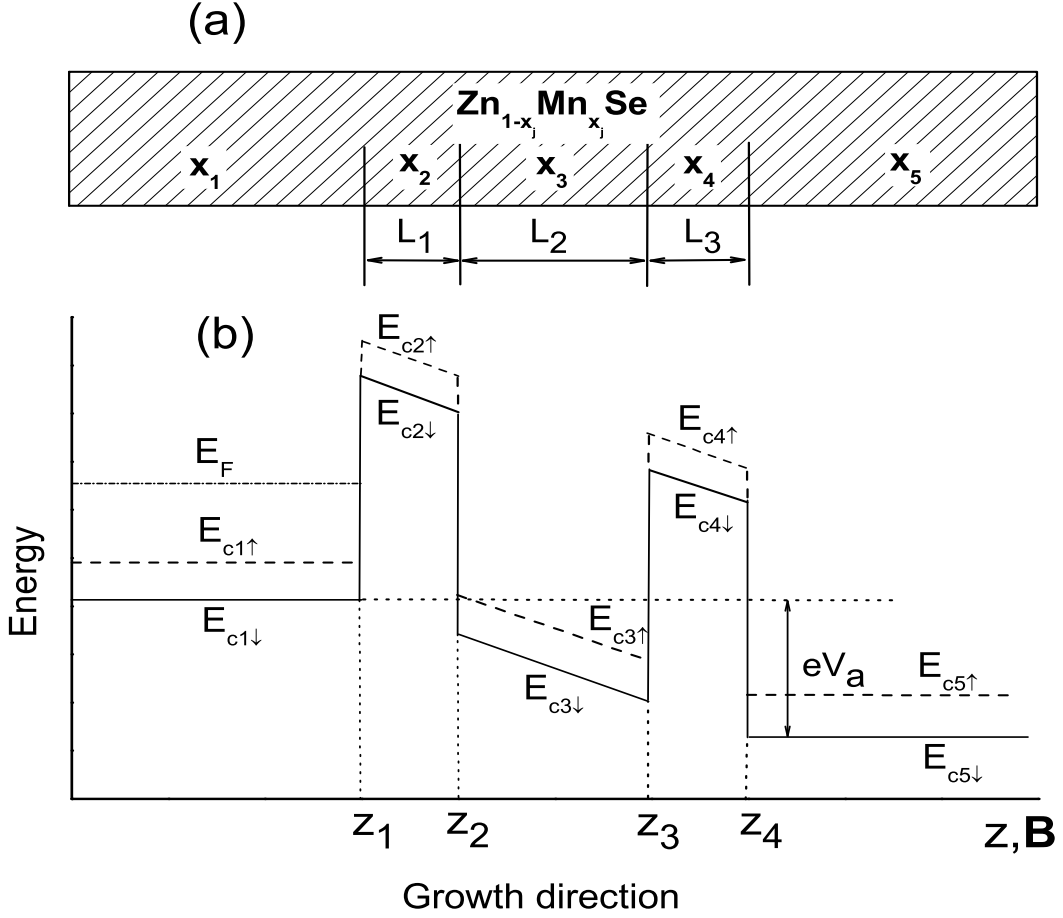


FIG. 1: (a) Zn<sub>1-x</sub>Mn<sub>x</sub>Se double-barrier resonant-tunnelling semimagnetic nanostructure (RTD) and (b) its spin-dependent conduction band profile in the nonzero magnetic field.

$$E_{c_j}(x_j) = \begin{cases} E_g(0), & x_j < 0.065, \\ E_0 + (1 - \text{VBO})x_j\Delta E_g & x_j > 0.065. \end{cases} \quad (1)$$

Here  $E_g(0) = 2.822$  eV is the band gap of ZnSe; VBO is the valence band offset;  $\Delta E_g = 0.4141$  eV,  $E_0$  is the fitting parameter (for each value of VBO, it is determined in such a way that at the point  $x_j = 0.065$  the function  $E_{c_j}(x_j)$  is continuous).

In the external magnetic field  $\mathbf{B}$ , the conduction band edge of the semimagnetic semiconductor is spin-dependent due to the effect of the giant Zeeman splitting of the electron energy levels [9, 10]. The value of the spin-dependent shift  $\epsilon_{j\sigma_z}(B)$  of the conduction band edge of the semimagnetic semiconductor is equal to the value of the energy of the  $sp-d$  ex-

change interaction between the conduction electrons and localized electrons of the magnetic Mn ions

$$\epsilon_{j\sigma_z}(B) = -\sigma_z x_j^{eff} N_0 \alpha \langle S_{zj} \rangle, \quad (2)$$

where  $\sigma_z = \pm 1/2$  (or  $\uparrow, \downarrow$ ) is the spin quantum number;  $x_j^{eff} = x_j(1 - x_j)^{12}$  is the effective concentration of Mn ions [4, 5, 6, 7, 8];  $N_0 \alpha$  is the *sp-d* exchange constant for conduction electrons; and  $\langle S_{zj} \rangle$  is the thermal average of the Mn spin component along the magnetic field  $\mathbf{B}$

$$\langle S_{zj} \rangle = -SB_S(g_{Mn}\mu_B SB/kT_j^{eff}). \quad (3)$$

Here  $B_S$  is the modified Brillouin function for the total spin quantum number of Mn ions;  $S = 5/2$ ;  $g_{Mn} = 2$  is *g*-factor of the spectroscopic splitting for Mn-*d*-electrons;  $\mu_B$  is the Bohr magneton;  $T_j^{eff} = T + T_j^{AF}$  is the effective temperature;  $T$  is the lattice temperature of semimagnetic semiconductors; and  $T_j^{AF}$  is the phenomenological parameter. The parameters,  $x_j^{eff}$  and  $T_j^{AF}$ , are required by the necessity to take into account the antiferromagnetic interaction between the Mn ions.

Thus, the conduction band edge of semimagnetic semiconductors  $E_{cj\sigma_z}$  in the magnetic field  $\mathbf{B}$  is determined by the following formula

$$E_{cj\sigma_z} = E_{cj} + \epsilon_{j\sigma_z}(B). \quad (4)$$

We consider sufficiently high magnetic fields for which the Landau quantization of transverse motion of electrons is important. Then the electron energy in each layer of the considered RTD has the following form:

$$E_{j\sigma_z} = E_{cj\sigma_z} + (l + \frac{1}{2})\hbar\omega_c + \sigma_z g^* \mu_B B + E_z. \quad (5)$$

Here  $l = 0, 1, 2, \dots$  is the Landau level quantum number;  $\omega_c = eB/cm^*$  is the electron cyclotron frequency;  $E_z = \hbar^2 k_z^2 / 2m^*$  is the electron energy connected with their motion along the RTD ( $k_z$  is the electron wave vector along  $z$  direction);  $m^*$  is the effective electron mass (we assume a single electron mass throughout all RTD layers); and  $g^*$  is the zone electron *g*-factor.

Taking into account expression (4), the electron energy in each RTD layer can be written in the following form

$$E_{j\sigma_z} = E_{gj} + (l + \frac{1}{2})\hbar\omega_c + \sigma_z g_j^{eff} \mu_B B + E_z, \quad (6)$$

where

$$g_j^{eff} = g^* + x_j^{eff} N_0 \alpha S B_S (g_{Mn} \mu_B S B / k T_j^{eff}) / \mu_B B. \quad (7)$$

The average current density through the RTD created by electrons with  $\sigma_z$  polarization in the magnetic field  $B$  at the finite temperature  $T$  is determined by the following expression [5, 6, 7]:

$$J_{\sigma_z} = J_0 B \sum_{l=0}^{\infty} \int_0^{\infty} T_{\sigma_z}(E_z, B, V_a) \{ f[E_z + (l + \frac{1}{2})\hbar\omega_c + \sigma_z g_1^{eff} \mu_B B] - f[E_z + (l + \frac{1}{2})\hbar\omega_c + eV_a + \sigma_z g_5^{eff} \mu_B B] \} dE_z, \quad (8)$$

where  $T_{\sigma_z}(E_z, B, V_a)$  is the electron transmission coefficient through the RTD;  $J_0 = e^2/h^2c$ ; and  $f(E) = 1/(1 + \exp((E - E_F)/kT))$  is the Fermi function.

The total current density  $J_t$  through the RTD is  $J_{\uparrow} + J_{\downarrow}$  and the coefficient of the current spin polarization  $P$  is

$$P = \frac{J_{\downarrow} - J_{\uparrow}}{J_{\downarrow} + J_{\uparrow}}. \quad (9)$$

To find  $T_{\sigma_z}(E_z, B, V_a)$  we use the Airy's-function-based transfer-matrix method [17]. This allows us to calculate  $J_{\sigma_z}$  numerically for arbitrary values of  $V_a$ . In the following we use these specific values of the RTD parameters:  $m^* = 0.16m_0$  ( $m_0$  is the free electron mass),  $g^* = 1.1$ ;  $N_0\alpha = 0.26$  eV;  $T=4.2$  K;  $T_{eff}^j = 2$  K;  $L_1 = L_3 = 5$  nm; and  $L_2 = 9$  nm. Note that the thicknesses of the quantum well and two barriers of the RTD correspond to the physical semimagnetic RTD with non-magnetic barriers, whose properties were investigated experimentally in [3].

## Numerical results and discussion

The spin-filtering effect of the electron current becomes most clearly apparent when the energy of the  $sp-d$  exchange interaction is maximal. Considering this energy as a function of  $x_j$ , it is easy to show from formula (2) that it is maximal at  $x_j = x_m = 1/13 \approx 0.077$ . Later on we will consider the case when the Mn concentration in the emitter and collector of the RTD is equal to this value, that is  $x_1 = x_5 = x_m$ . This allows us to obtain the maximal value of the spin-dependent shift of the conduction band edge of the emitter and collector. To create the potential profile inherent in double-barrier RTDs, it is required that the concentration of Mn ions in the two barriers ( $x_2$  and  $x_4$ ) is larger than in the emitter

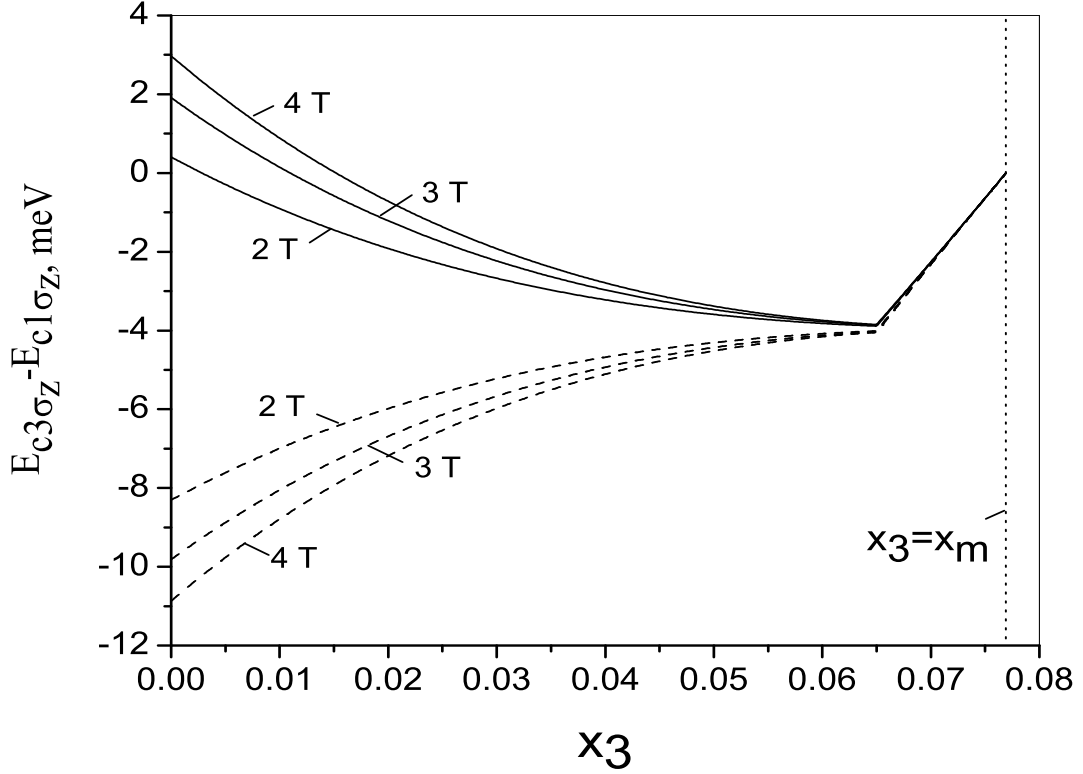


FIG. 2: Dependence of the conduction-band edge of the RTD quantum well on the Mn-ion concentration  $x_3$  for spin-down (solid lines) and spin-up (dashed lines) electrons for  $B = 2, 3, 4$  T.

( $x_1$ ), collector ( $x_5$ ), and the potential well ( $x_3$ ). We assume that  $x_2 = x_4 = 0.25$ , and  $x_3$  is changed from  $x_3 = 0$  to  $x_3 = x_m$ .

#### A. The spin-dependent RTD conduction band profile at the zero bias voltage

Fig.2 shows the dependence of the spin-dependent conduction band edge of the RTD quantum well on the Mn concentration  $x_3$  for three values of  $B = 2, 3, 4$  T. In this case, we choose the zero of the energy to be at the conduction band edge of the RTD emitter (the solid lines correspond to the spin-down electrons and the dashed lines correspond to the spin-up electrons). It is seen from Fig.2 that with increasing  $B$ , the difference in the position of the conduction band edges of the RTD quantum well for the spin-up and spin-down electrons increases. At a fixed value of  $B$ , the largest difference in the position of the spin-dependent conduction band edges takes place, and hence the largest spin splitting of

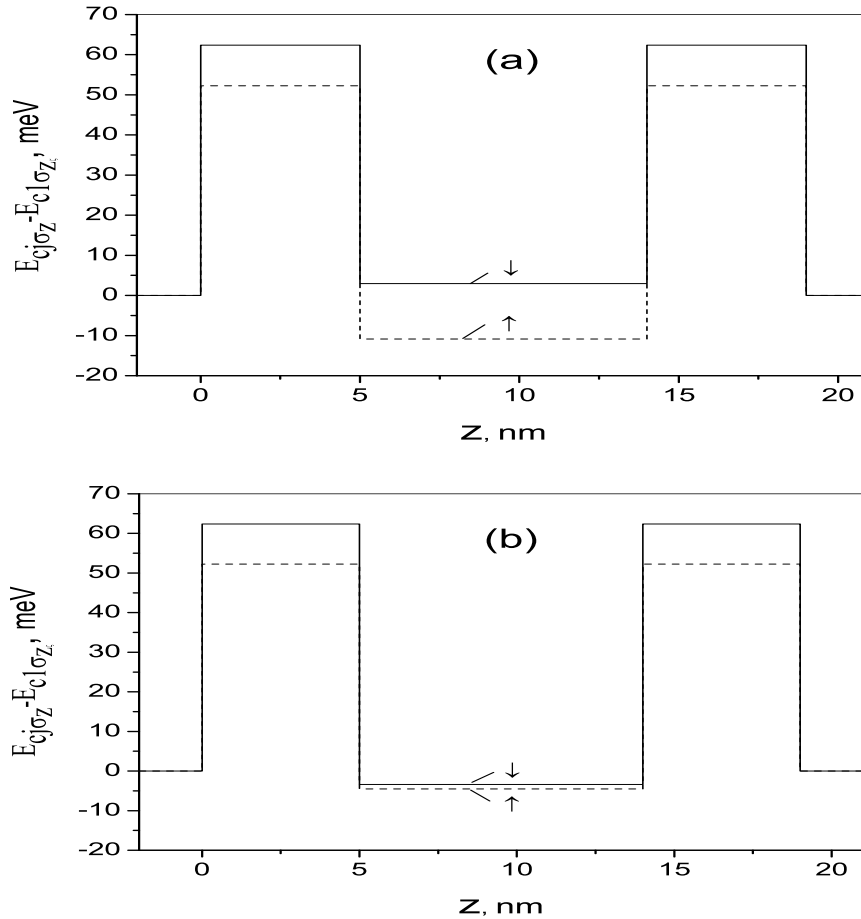


FIG. 3: The zero bias voltage RTD potential profile for spin-down electrons (solid lines) and for spin-up electrons (dashed lines) for (a)  $x_3 = 0.0$  and (b)  $x_3 = 0.05$  at  $B = 4$  T.

the electron levels in the RTD quantum well occurs, at  $x_3 = 0$ . For this reason we begin our study of the value of the total RTD current density  $J_t$  and the value of the coefficient of the RTD current spin polarization  $P$  with this case.

Fig.3 shows the zero bias voltage RTD potential profile (the energy is measured from the conduction band edge of the emitter,  $z_1 = 0$ ) for spin-down electrons (solid lines) and for spin-up electrons (dashed lines) for (a)  $x_3 = 0.0$  and (b)  $x_3 = 0.05$  at  $B = 4$  T. One can see that for spin-up electrons the barriers are smaller and the quantum well is deeper than for spin-down electrons. Consequently, the energy levels in the quantum well lie deeper for spin-up electrons than for the spin-down electrons. It is obvious that with decreasing  $x_3$ , the difference in the potential profile for spin-up and spin-down electrons increases, and the



effect of electron current spin filtering becomes more apparent.

### B. Magnetic field dependencies of the RTD current spin polarization

In Fig.4 the dependencies of  $J_{\uparrow}(V_a)$ ,  $J_{\downarrow}(V_a)$ ,  $J_t(V_a)$  (the left axis of ordinates) and  $P(V_a)$  (the right axis of ordinates) are shown at (a)  $B = 2$  T and (b)  $B = 4$  T for  $x_3 = 0.0$  and  $E_F = 10$  meV. It is seen from these figures that there are two current density peaks in the curves  $J_{\uparrow}(V_a)$  and  $J_{\downarrow}(V_a)$ . With increasing  $B$ , the values of the peaks of  $J_{\downarrow}(V_a)$  increase and for  $J_{\uparrow}(V_a)$  they decrease. In this case, the values of the peaks of the total current density  $J_t(V_a)$  increase when  $B$  increases. The dependencies of  $P(V_a)$  are non-monotone functions and the values of the peaks of  $P$  rise with increasing  $B$  as well. The low-voltage range is of interest, in which  $P \approx 1$  for the relatively small value of  $B = 2$  T. In Fig.4, the presence of two peaks of the current densities  $J_{\downarrow}(V_a)$  and  $J_{\uparrow}(V_a)$  corresponds to the two lowest resonant spin splitting electron energy levels in the RTD quantum well. In this case, as the bias voltage increases the resonant electron transmission takes place, from the beginning, for the first lowest electron energy level in the quantum well and then for the second electron energy level. Note that the shape of the first peak in  $J_t(V_a)$  has interesting features such as at  $B = 2$  T the current density peak is split and at  $B = 4$  T there are kinks. This is due to both the presence of the spin splitting of the electron energy levels in the quantum well and the quantization of the transverse electron motion (the presence of the Landau levels).

A note should be made concerning the physical phenomena determining the shape of the above-mentioned dependencies  $J_t(V_a)$  and  $P(V_a)$ . For this reason we plot  $T_{\downarrow}(E_z)$  (Fig.5a) and  $T_{\uparrow}(E_z)$  (Fig.5b) for the different values of the voltage bias  $V_a$  for  $B = 4$  T and  $x_3 = 0.0$  (the numbers next to the curves show the corresponding values of  $V_a$  in volts).

There are resonant peaks with unit peak-value in  $T_{\downarrow}(E_z)$  and  $T_{\uparrow}(E_z)$  for  $V_a = 0$  (in view of the chosen scale in Fig.5, these curves show only the region of the first resonant peak both for  $T_{\downarrow}(E_z)$  and for  $T_{\uparrow}(E_z)$ ). Due to the fact that the depth of the potential well depends significantly on the electron spin, the resonant peaks of  $T_{\downarrow}(E_z)$  and  $T_{\uparrow}(E_z)$  strongly differ in location. With increasing  $V_a$  the resonant peaks of  $T_{\downarrow}(E_z)$  and  $T_{\uparrow}(E_z)$  shift in the low-energy region, and their peak values decrease. In Fig.5 and Fig.6 the dotted lines show the values of

$$E_{zm}^{\sigma z}(l) = E_F - \frac{1}{2}\hbar\omega_c - \sigma_z g_1^{eff} \mu_B B, \quad (10)$$

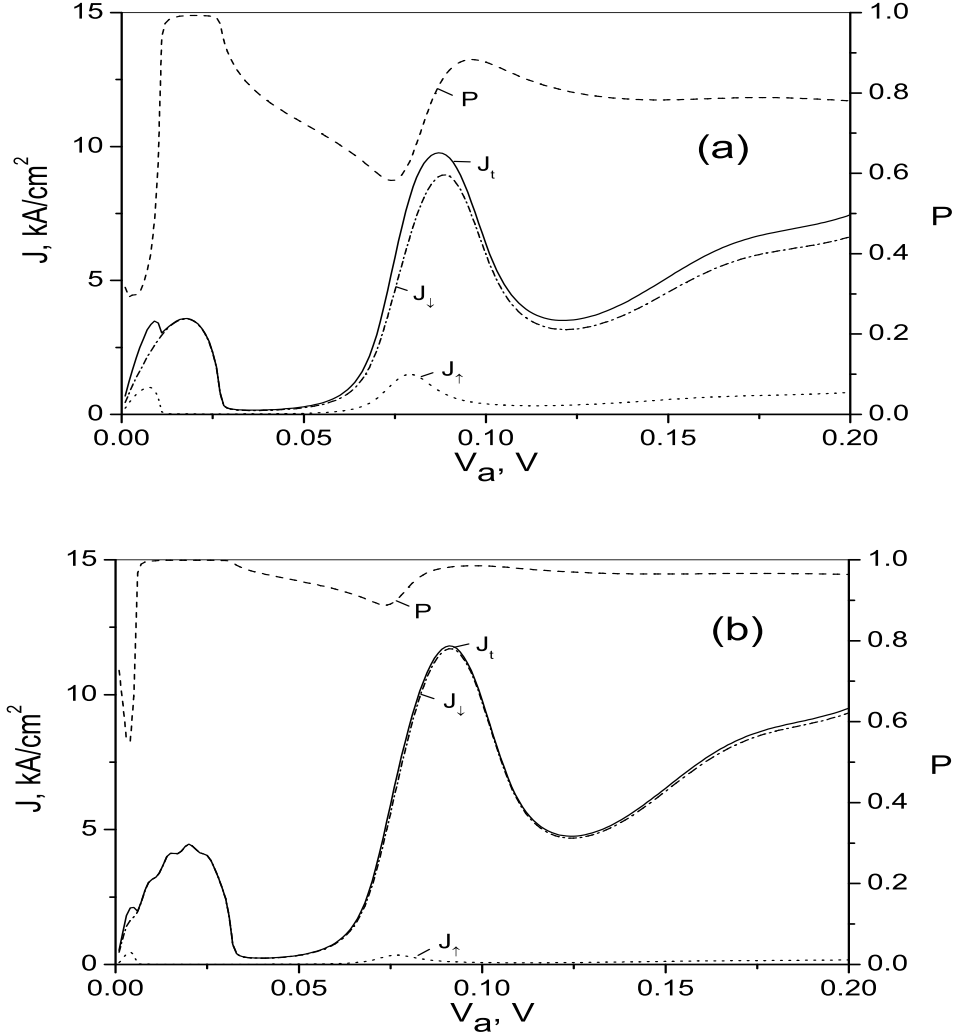


FIG. 4:  $J_{\uparrow}(V_a)$ ,  $J_{\downarrow}(V_a)$ ,  $J_t(V_a)$  (the left axis of ordinates) and  $P(V_a)$  (the right axis of ordinates) at (a)  $B = 2$  T and (b)  $B = 4$  T for  $x_3 = 0.0$ ,  $E_F = 10$  meV.

which are the maximal values of the longitudinal electron energy  $E_z$  for each Landau level  $l$ . The electrons located at Landau level  $l$  pass through the RTD when  $E_{zm}^{\sigma_z}(l) > 0$ . For  $\sigma_z = 1/2$ , this condition is fulfilled only for  $l = 0$ , but at  $\sigma_z = -1/2$  it holds for  $l = 0, \dots, 5$ . With increasing  $V_a$  the current through the RTD occurs as soon as the first resonant peak of  $T_{\sigma_z}$  intersects the line  $E_z = E_{zm}^{\sigma_z}(0)$  for the Landau level,  $l = 0$ . For spin-down electrons this takes place at  $V_a = 0.002$  V and for the spin-up electrons it occurs at  $V_a = 0.0026$  V. It is seen from Fig.5a that with increasing  $V_a$  the resonant peak of  $T_{\downarrow}(E_z)$  shifts towards the

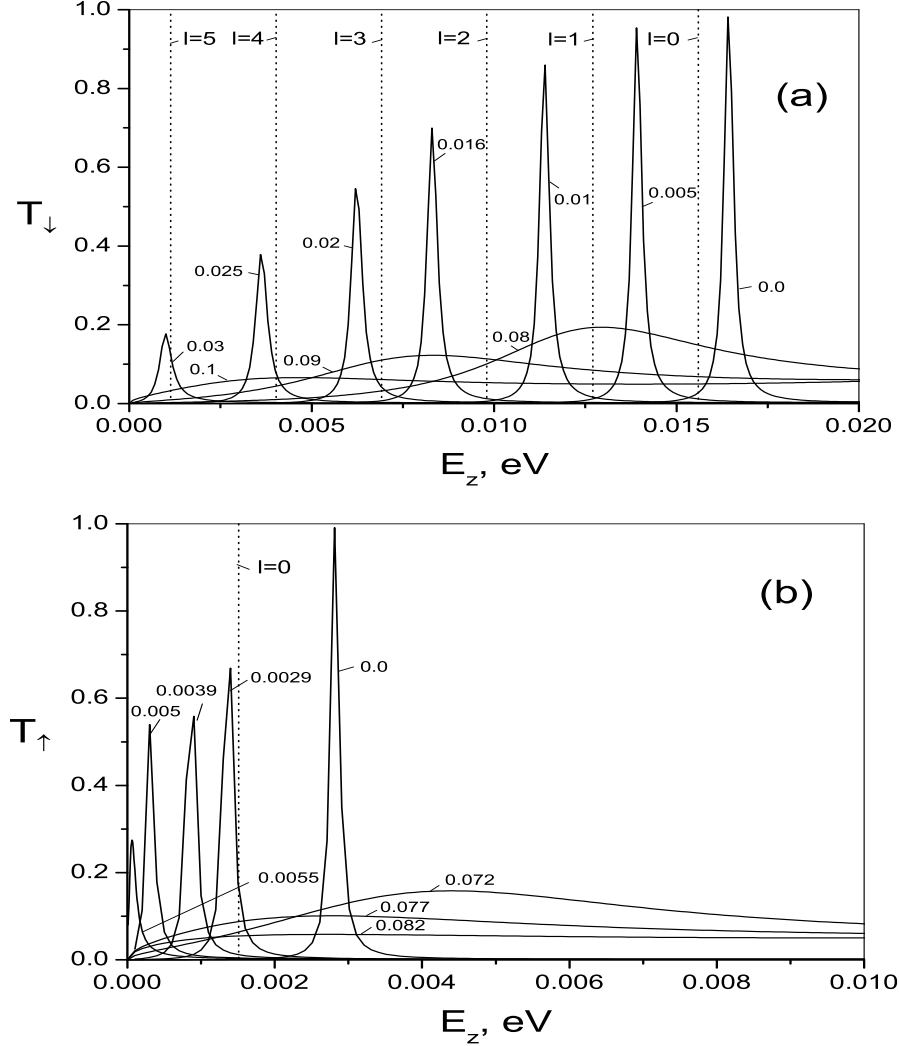


FIG. 5: (a)  $T_{\downarrow}(E_z)$  and (b)  $T_{\uparrow}(E_z)$  for the different values of the voltage bias  $V_a$  at  $B = 4$  T and  $x_3 = 0.0$  (the numbers next to the curves show the corresponding values of  $V_a$  in volts).

low-energy region. In this case, the resonant peak decreases in magnitude and successively intersects the lines  $E_z = E_{zm}^{\sigma_z}(l)$ . At each intersection, the current density  $J_{\downarrow}$  increases at the expense of the electrons located at the corresponding Landau levels  $l$ , and a kink in  $J_{\downarrow}(V_a)$  occurs. On the other hand, the decrease in the magnitude of the resonant peak of  $T_{\downarrow}$  leads to a decrease in  $J_{\downarrow}$ . At a fixed value of  $V_a$ , the magnitude of  $T_{\downarrow}(E_z)$  decreases so much that electrons with all possible values of  $l$  give a very small contribution to the current, and it becomes minimal. At  $\sigma_z = 1/2$  the current density  $J_{\uparrow}$  is only determined by electrons

with  $l = 0$ , so the contribution of this current component to the total current density  $J_t$  is small. With a further increase in  $V_a$ , the second resonant peak of  $T_{\sigma_z}(E_z)$  intersects the line  $E_{zm}^{\sigma_z}(0)$ , and a second peak appears in  $J_{\downarrow}(V_a)$  and  $J_{\uparrow}(V_a)$ . In this case, the width of the second peak of  $T_{\downarrow}(E_z)$  is so large that it intersects practically all lines  $E_{zm}^{\downarrow}(l)$  (at  $V_a \geq 0.08$  V). As a result,  $J_{\downarrow}$  is produced by the electrons located at all the filled Landau levels. For this reason the second peak of  $J_{\downarrow}(V_a)$  is higher and smoother than first one, and it does not contain visible kinks. Note that the value of the second peak of  $J_{\uparrow}$  approximately equals to the value of the first peak.

Let us denote the resonant peak locations of  $T_{\sigma_z}(E_z)$  by  $E_{zp}^{\sigma_z}$ . Fig.6 shows the dependencies of  $E_{zp}^{\sigma_z}(V_a)$  for the first two peaks of  $T_{\downarrow}(E_z)$  (solid lines) and  $T_{\uparrow}(E_z)$  (dashed lines) for  $B = 4$  T,  $E_F = 10$  meV, and  $x_3 = 0.0$ . It is seen from this figure that the first and second resonant peaks of  $T_{\downarrow}(E_z)$  are located in the region of smaller values of  $E_z$  than those of  $T_{\uparrow}(E_z)$ . With increasing  $V_a$ , the locations of the resonant peaks of  $T_{\sigma_z}(E_z)$  shift to the low-energy region. Each current density component  $J_{\sigma_z}$  makes a contribution to the total current density  $J_t$  for those values of  $V_a$  for which the value of  $E_{zp}^{\sigma_z}$  is less than the value of  $E_{zm}^{\sigma_z}(0)$ . Note that the end-points of the  $E_{zp}^{\sigma_z}(V_a)$  dependencies correspond to the disappearance of the resonant peaks in the  $T_{\sigma_z}(E_z)$ , i.e. these dependencies are monotone with further increase of  $V_a$ .

### C. The effect of total RTD current spin polarization

It is clear that a high degree of the current spin polarization occurs when  $J_{\uparrow}$  is small. It follows from (8) that at low temperatures the current is only created by the electrons for which the condition  $E_z < E_{zm}^{\sigma_z}(l)$  is fulfilled. It is obvious that for the spin-up electrons ( $\sigma_z = 1/2$ ) located at the lowest Landau level ( $l = 0$ ), the condition  $E_{zm}^{\uparrow}(0) \leq 0$  can be fulfilled. This implies that for the spin-up electrons, the lowest Landau level is located higher than the Fermi level, and spin-up electrons are absent in the RTD emitter. As a result, the effect of total spin polarization of the electron current in the RTD must occur when the current is only caused by the spin-down electrons ( $J_{\uparrow} = 0$ ,  $P = 1$ ).

Let us show that the condition  $E_{zm}^{\uparrow}(0) \leq 0$  can be fulfilled for moderate magnetic fields  $B$ . In Fig.7 the  $E_F(B)$  dependence (solid curve 1), corresponding to the solution of equation  $E_{zm}^{\uparrow}(0) = 0$ , is plotted along the left axis of the ordinates. The magnetic field dependence of

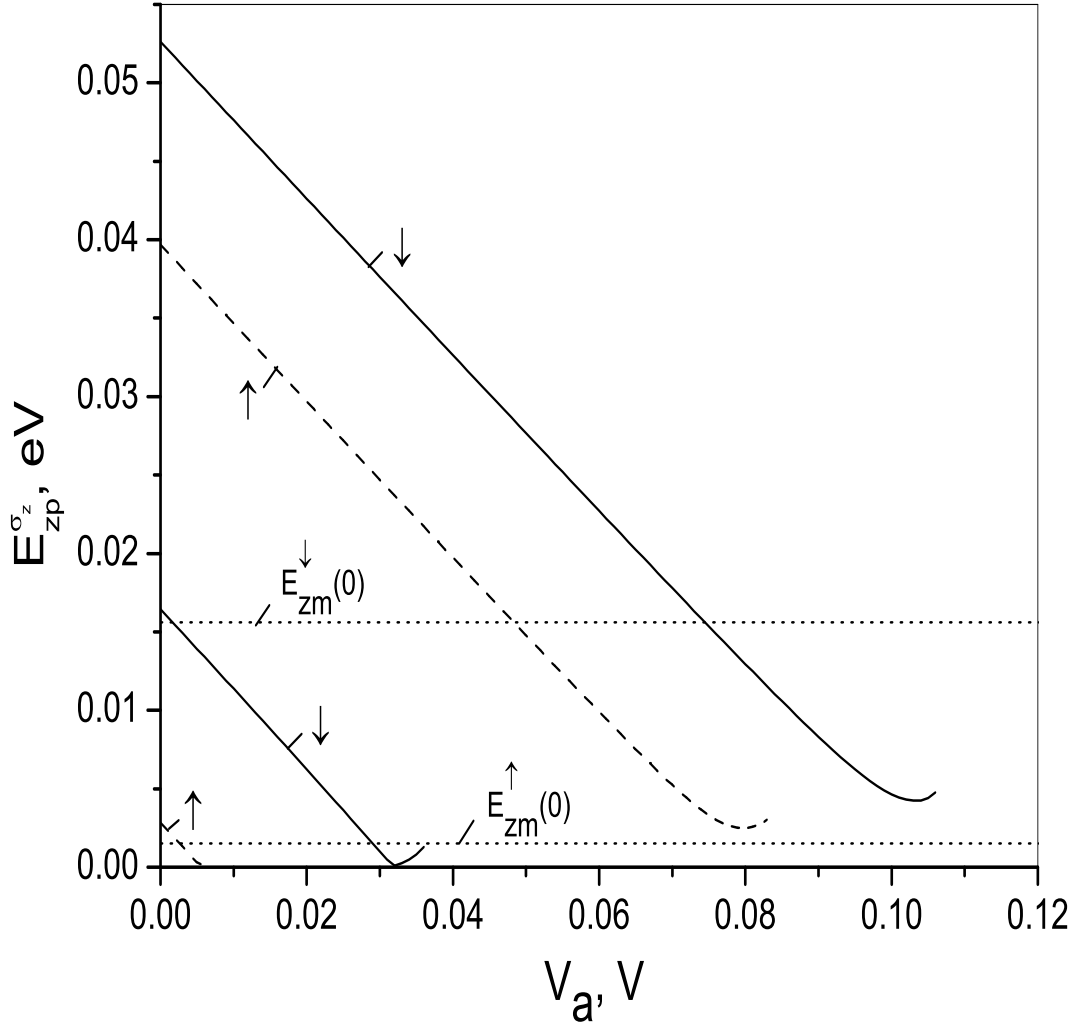


FIG. 6: The bias-voltage dependence of the locations  $E_{zp}^{\sigma_z}$  of two resonant peaks in the dependencies  $T_{\downarrow}(E_z)$  (solid lines) and  $T_{\uparrow}(E_z)$  (dashed lines) for  $B = 4$  T and  $x_3 = 0.0$ .

the RTD emitter electron concentration  $n$  (dashed curve 2) is presented along the right axis of the ordinates assuming that  $n$  is related to  $E_F$  by the equation  $n = (1/3\pi^2)(2m^*E_F/\hbar^2)^{3/2}$ . (We consider the electron gas in the RTD emitter to be degenerate). For a fixed value of  $E_F$ , the effect of the total spin polarization of the electron current must occur starting at a critical value of  $B$ . (This situation corresponds to the dashed area in Fig.7). Note that in order to decrease the critical value of  $B$ , it is necessary to decrease the value of  $E_F$ . For example, for the moderate value  $B = 2$  T the effect of the total spin polarization of the

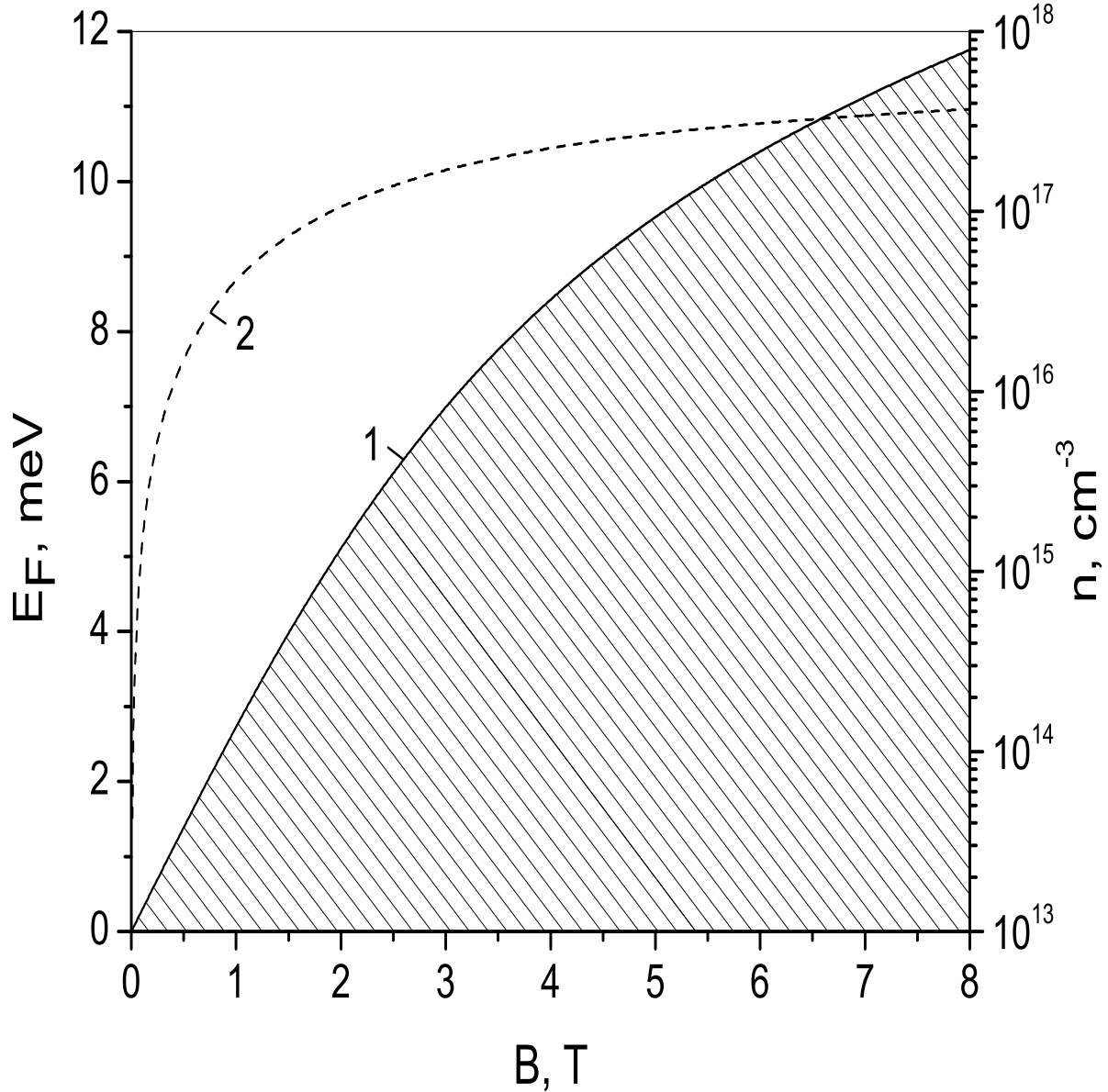


FIG. 7:  $E_F(B)$  (left ordinate axis) and  $n(B)$  (right ordinate axis) corresponding to the occurrence of total current spin polarization effect.

electron current occurs at  $E_F = 5.1$  meV. (The corresponding value of  $n$  is  $10^{17}$   $\text{cm}^{-3}$ ).

Now we consider the influence of constant magnetic field  $B$  on the  $J_t(V_a)$  and  $P(V_a)$  for two values of the Mn concentration  $x_3$  in the RTD quantum well at  $E_F = 5.1$  meV. In Fig.8  $J_t(V_a)$  (the left axis of ordinates, curves of different types except dashed lines) and  $P(V_a)$  (the right axis of ordinates, dashed lines) are shown for (a)  $x_3 = 0.0$ , (b)  $x_3 = 0.05$  for five different values of  $B = 0.5, 1, 2, 3, 4$  T. It is seen from Fig.8 that with increasing  $B$  the current density  $J_t$  in the RTD increases, and kinks on the first resonant peak of  $J_t$  arise.

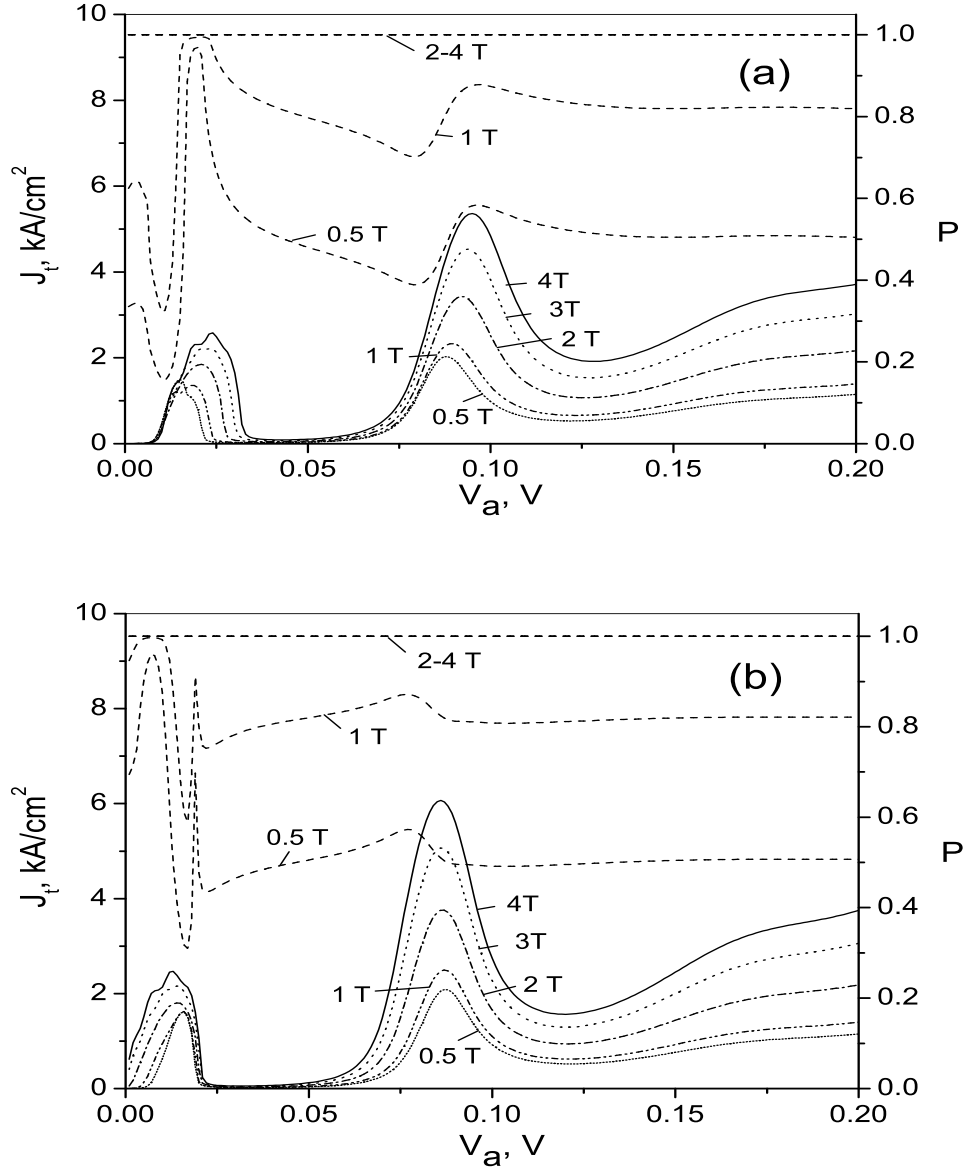


FIG. 8:  $J_t(V_a)$  (the left axis of ordinates) and  $P(V_a)$  (the right axis of ordinates) for five values of  $B = 0.5, 1, 2, 3, 4$  T,  $E_F = 5.1$  meV at (a)  $x_3 = 0.0$  and (b)  $x_3 = 0.05$ .

The value of  $P$  also increases with increasing  $B$ . Starting with  $B = 2$  T the electron current in the RTD is totally spin polarized ( $P = 1$ ). As one can see in Fig.8a, in the case  $x_3 = 0.0$  the peaks of the  $J_t(V_a)$  coincide with the peaks of  $P(V_a)$ . For the case  $x_3 = 0.05$  (Fig.8b) the situation is different because the peak values of the current density correspond to the

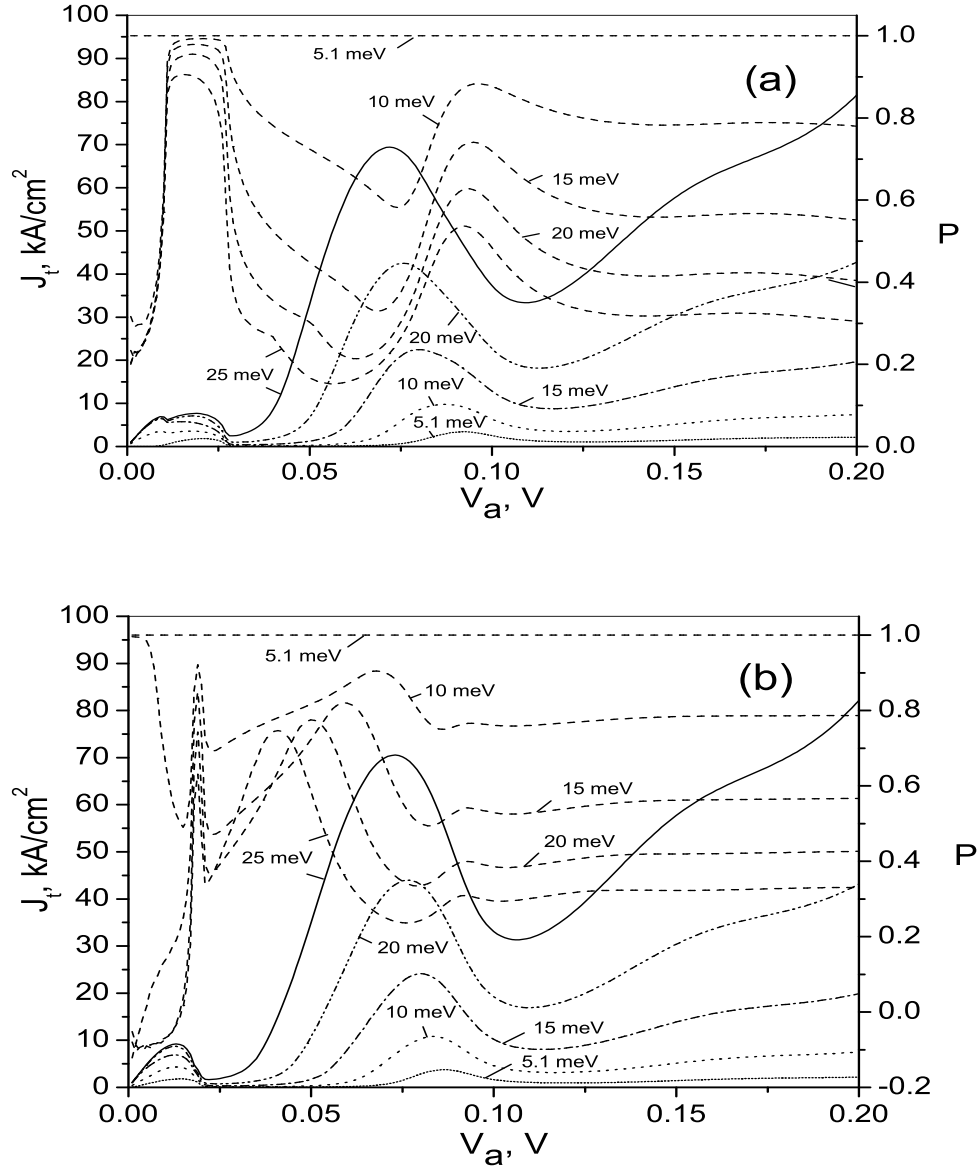


FIG. 9:  $J_t(V_a)$  (the left axis of ordinates) and  $P(V_a)$  (the right axis of ordinates) for five values of  $E_F = 5.1, 1, 2, 3, 4$  meV,  $B = 2$  T at (a)  $x_3 = 0.0$  and (b)  $x_3 = 0.05$ .

local minima of  $P$ . So, we conclude that in moderately low magnetic fields  $B$ , the maximal degree of the current spin polarization in the peak values of the current takes place when the RTD quantum well does not contain Mn ions. In this case the first current density peak is characterized by almost total current spin polarization.



In order to obtain a high value of the spin-polarized current in the RTD, it is necessary to increase  $E_F$ . Fig.9 shows  $J_t(V_a)$  (the left axis of ordinates, curves of different types except dashed lines) and  $P(V_a)$  (the right axis of ordinates, dashed lines) at (a)  $x_3 = 0.0$  and (b)  $x_3 = 0.05$  for five different values of  $E_F = 5.1, 10, 15, 20, 25$  meV at  $B = 2$  T. It is seen from Fig.9 that with increasing  $E_F$  the current density peak values increase. However, the value of  $P$  decreases and, moreover, the function  $P$  becomes negative in low-voltage region for the case  $x_3 = 0.05$  (Fig.9b). The first current density peak is characterized by the high value of  $P$  for the case  $x_3 = 0.0$  as usual, but the difference in  $P$  for the second peak in cases  $x_3 = 0.0$  and  $x_3 = 0.05$  becomes smaller. Note that the high value of the peak-to-valley ratio typical of the first current density peak also decreases with increasing  $E_F$ .

### Conclusion

In this paper, we have investigated theoretically the spin-polarized electron current in a double-barrier semimagnetic RTD based entirely on  $\text{Zn}_{1-x}\text{Mn}_x\text{Se}$  semimagnetic semiconductor. We have demonstrated the dependence of the current spin polarization on the external constant magnetic field, the applied voltage bias, and the distribution of Mn ions in the RTD. We have obtained the condition for total current spin polarization in the semimagnetic RTD, and we have found the optimal distribution of Mn ions in the RTD providing the maximal current spin polarization in the current peaks for arbitrary values of the external magnetic fields and the Fermi levels in the RTD emitter. We have demonstrated that the degree of current spin polarization in the semimagnetic RTD can be effectively controlled by an electric field, and this fact can be used for creating the voltage controlled sources of spin polarized current for spintronics devices.

### Acknowledgments

We are grateful to G. D. Doolen for useful discussions. This work was supported by the Department of Energy (DOE) under Contract No. W-7405-ENG-36, by the National

Security Agency (NSA), and by the Advanced Research and Development Activity (ARDA).

---

- [1] R. Wessel, L. D. Vagner. Superlattices and Microstructures **8**, 443(1990).
- [2] V. A. Chitta, M. Z. Maialle, S. A. Leao, M. H. Degani. Appl. Phys. Lett. **74**, 2845 (1999).
- [3] A. Slobodskyy, C. Gould, T. Slobodskyy, C. R. Becker, G. Schmidt, L.W.Molenkamp. Phys. Rev. Lett., **90**, 246601 (2003).
- [4] J. C. Egues. Phys. Rev. Lett. **80**, 4578 (1998).
- [5] Y. Guo, H. Wang, B.-L. Gu, Y. Kawazoe. J. Appl. Phys. **88**, 6614 (2000).
- [6] Y. Guo, B.-L. Gu, H. Wang, Y. Kawazoe. Phys. Rev. B **63**, 214415 (2001).
- [7] Y. Guo, J.-Q. Lu, Z. Zeng, Q. Wang, B.-L. Gu, Y. Kawazoe. Phys. Lett. A **284**, 205 (2001).
- [8] J. C. Egues, C. Gould, G. Richter, L. W. Molenkamp. Phys. Rev. B **64**, 195319 (2001).
- [9] J. K. Furdyna. J.Appl.Phys., **64**, R29 (1988).
- [10] O. Goede, W. Heimbrodt. Phys.Stat.Sol.(b), **146**, 11 (1988).
- [11] Eunsoon Oh, D. U. Bartholomew, A. K. Ramdas, J. K. Furdyna, U. Debska. Phys. Rev. B, **44**, 10551 (1991).
- [12] R. Fiederling, M. Keim, G. Reuscher, W. Ossau, G. Schmidt, A.Waag, and L. W. Molenkamp. Nature, **402**, 787 (1999).
- [13] B. T. Jonker, Y. D. Park, B. R. Bennett, H. D. Cheong, G. Kioseoglou, A. Petrou. Phys. Rev. B, **62**, 8180 (2000).
- [14] P. J. Klar, D. Wolverson, J. J. Davies, W. Heimbrodt, M. Happ. Phys. Rev. B, **57**, 7103 (1998).
- [15] R. B. Bylsma, W. M. Becker, J. Kossut, U. Debska, D. Yoder-Short. Phys. Rev. B, **33**, 8207 (1986).
- [16] A. A. Toropov, A.V. Lebedev, S. V. Sorokin, D. D. Solnyshkov, S. V. Ivanov, P. S. Kopev, I. A. Buyanova, W. M. Chen, and B. Monemar. Semiconductors, **36**, 1288 (2002).
- [17] S. Vatannia, G. Gindenblat. IEEE J. Quantum Electron. **32**, 1093 (1996).

## Figure captions

**Fig.1** (a)  $\text{Zn}_{1-x}\text{Mn}_x\text{Se}$  double-barrier resonant-tunnelling semimagnetic nanostructure (RTD) and (b) its spin-dependent conduction band profile at the nonzero bias voltage.

**Fig.2** Dependence of the conduction-band edges of the RTD quantum well on the Mn ion concentration  $x_3$  for spin-down (solid lines) and spin-up (dashed lines) electrons for  $B = 2, 3, 4$  T.

**Fig.3** The zero bias voltage RTD potential profile for spin-down electrons (solid lines) and for spin-up electrons (dashed lines) for (a)  $x_3 = 0.0$  and (b)  $x_3 = 0.05$  at  $B = 4$  T.

**Fig.4**  $J_\uparrow(V_a)$ ,  $J_\downarrow(V_a)$ ,  $J_t(V_a)$  (the left axis of ordinates) and  $P(V_a)$  (the right axis of ordinates) at (a)  $B = 2$  T and (b)  $B = 4$  T for  $x_3 = 0.0$ ,  $E_F = 10$  meV.

**Fig.5** (a)  $T_\downarrow(E_z)$  and (b)  $T_\uparrow(E_z)$  for the different values of the voltage bias  $V_a$  at  $B = 4$  T and  $x_3 = 0.0$  (the numbers next to the curves show the corresponding values of  $V_a$  in volts).

**Fig.6** The bias-voltage dependence of the  $E_{zp}^{\sigma_z}$  locations of two resonant peaks in the dependencies  $T_\downarrow(E_z)$  (solid lines) and  $T_\uparrow(E_z)$  (dashed lines) for  $B = 4$  T and  $x_3 = 0.0$ .

**Fig.7**  $E_F(B)$  (left ordinate axis) and  $n(B)$  (right ordinate axis) corresponding to occurrence of the total current spin polarization effect.

**Fig.8**  $J_t(V_a)$  (the left axis of ordinates) and  $P(V - a)$  (the right axis of ordinates) for five values of  $B = 0.5, 1, 2, 3, 4$  T,  $E_F = 5.1$  meV at (a)  $x_3 = 0.0$  and (b)  $x_3 = 0.05$ .

**Fig.9**  $J_t(V_a)$  (the left axis of ordinates) and  $P(V - a)$  (the right axis of ordinates) for five values of  $E_F = 5.1, 1, 2, 3, 4$  meV,  $B = 2$  T at (a)  $x_3 = 0.0$  and (b)  $x_3 = 0.05$ .